Void plasmons and total absorption of light in nanoporous metallic films

T. V. Teperik and V. V. Popov
Institute of Radio Engineering and Electronics (Saratov Division), Russian Academy of Sciences, Saratov 410019, Russia

F. J. García de Abajo
Centro Mixto Consejo Superior de Investigaciones Científicas–Universidad del País Vasco/Euskal Herriko Universitatea and Donostia International Physics Center, Aptdo. 1072, 20080 San Sebastian, Spain

(Received 1 August 2004; revised manuscript received 17 November 2004; published 9 February 2005)

We have calculated light absorption spectra of planar metal structures containing a two-dimensional (2D) lattice of spherical nanocavities. Two types of porous metal structures are considered: (i) unsupported planar metal films containing a lattice of voids and (ii) planar metal films with a lattice of voids supported by the bulk metal substrate. It is shown that nearly total absorption of light occurs at the plasma resonance of the void lattice in the visible when the intervoid spacing and the void deepening into the bulk metal substrate are thinner than the skin depth, which ensures optimal coupling of void plasmons to external light. It is remarkable that even a single 2D lattice of nanovoids beneath the planar metal surface can produce the total light absorption. This giant light absorption is accompanied by strong local-field enhancement at the plasma resonance. The absorption and local-field properties of these types of nanoporous metal structures can be effectively tuned by nanoengineering the spherical pores.

DOI: 10.1103/PhysRevB.71.085408 PACS number(s): 73.20.Mf, 61.46.+w, 78.20.Bh

I. INTRODUCTION

Planar metal surfaces absorb light very poorly in general. The reason for this can be found in their high free-electron density, which reacts to the incident light by sustaining strong oscillating currents that, in turn, reradiate light efficiently back into the surrounding medium, whereas the light intensity inside metal remains weak. Actually, the same phenomenon takes place when light excites plasma oscillations in metallic particles. As a result, the local-field enhancement inside or near the particles appears to be quite moderate even at the plasma resonance (e.g., local-field enhancement factors up to 15 have been reported for spherical metallic nanoparticles[1,2]).

In apparent contradiction with the above arguments, strong (up to −20 dB) resonant dips in the reflectivity spectra of light have been recently observed[3] at oblique incidence from nanoporous gold surfaces formed by periodical arrangements of close-packed spherical segment voids (nanocups). Since there is no transmission through the metal substrate, these resonant peaks indicate the presence of strong resonant absorption on such surfaces.

It was presumed in Ref. 3 that this phenomenon is related to the excitation of plasmon modes in nanocups, which couple much more effectively to the light than those in, e.g., metallic spheres. As an intuitive explanation of their observations, the authors of Ref. 3 employed a simple model of plasmon modes supported by a spherical void in an infinite metallic medium. Although that model gives eigenfrequency values that somehow can be fitted to the frequencies of the resonances in the measured reflectivity spectra, it cannot describe the coupling between plasmon modes in the nanocavity and the external radiation field. The reason is that the plasmon modes in a void are nonradiative because their electromagnetic field cannot radiate into an infinite metal having a negative permittivity. However, the huge resonant dips in the reflectivity spectra that were observed in Ref. 3 suggest effective coupling of nanocavity plasmons to the incident light. Therefore, a better understanding of the effect of coupling between plasmons in metallic nanocavities and external radiation becomes important.

In Refs. 4 and 5 the reflectivity spectra of close-packed segment voids in metallic films were experimentally studied for normal incidence of light; however, only moderate dips in the reflectivity spectra were observed. The authors of Ref. 4 and 5 described their experimental observations by making use of a simple optical ray model. While this theoretical model explains satisfactorily the optical properties of the shallow cups of large diameter (up to 10 μm) studied in the experiments,[4,5] it obviously becomes invalid for nanocups with smaller diameters comparable to the light wavelength, for which ray optics is not applicable because it takes into account only the geometrical aspect of the problem but neglects plasmons confined in every nanocup as well as diffraction phenomena in the lattice of nanocups altogether.

In this context, it has been shown in Refs. 6–8 that the spectra of plasma oscillations in spherical metallic nanoparticles with inner voids (nanoshells) are much richer than those in solid metallic nanospheres. Both spherelike plasmons (those mainly bound to the outer surface of the shell) and void-like plasmons (bound to the inner surface) can be excited in such particles. Optical properties of a single metallic nanoshell and nanoshell clusters can be effectively tuned by nano-engineering their geometry. As it has been theoretically shown in Ref. 8, the local-field enhancement factor at the void-like plasmon resonance can reach ultrahigh values for a specific thickness of the shell layer, accompanied by sharply enhanced light absorption at the resonance.[8] Such local-field enhancement at the plasma resonances on metal surfaces with negative curvature may be relevant to the enhanced Raman scattering of light by molecules absorbed at those surfaces when they exhibit compli-

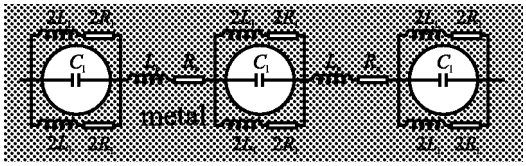

FIG. 1. Lattice of voids and its equivalent circuit.

cated profiles.[9] References 10 and 11, where enhanced light absorption in a slab of metallic nanoporous photonic crystal has been theoretically studied, also should be referred to in this connection.

In this paper, we study the optical plasmonic properties of hexagonal two-dimensional (2D) lattices of spherical nanovoids inside metals. In Sec. II, we start with a simple model of the resonant surface layer that captures the essential physics underlying unusual optical properties of the void lattice buried in metal. We consider two types of structures: (i) unsupported planar metal films containing a lattice of voids and (ii) planar metal films with a lattice of voids supported by the bulk metal substrate (i.e., the lattice of voids lies right beneath the planar surface of the metal). In Sec. IV, we corroborate the results derived from our simple model of Sec. II by comparing them with transmission and absorption spectra of nanoporous metal structures calculated in the framework of a self-consistent electromagnetic multiple-scattering layer–Korringa-Kohn-Rostoker (KKR) approach,[12–14] which is briefly described in Sec. III and which allows us to take into account the actual structure of void lattice. We show that the frequencies of absorption resonances can be effectively tuned by varying the diameter of the voids or by filling them with different dielectric materials. We also estimate the local-field enhancement factor at the plasma resonances of the void lattice and show that enhanced resonant light absorption is accompanied by strong local-field enhancement. The conclusions are summarized in Sec. V.

II. SIMPLE MODEL FOR A RESONANT SURFACE LAYER

A. Effective surface impedance of a void lattice in metal

In order to examine the essential physics of energy transformation in the system, we elaborate in this section a simple model describing a 2D lattice of voids in metal (Fig. 1) by its equivalent impedance Z_{eff}. In this section, we use the local Drude model to describe the conductivity of the metal,

$$\sigma_e(\omega) = \frac{e^2 N_e}{m(\nu_e - i\omega)},$$

where N_e is the bulk free-electron density, ν_e is the free-electron scattering rate, and e and m are the electron charge and mass, respectively. For a planar surface of homogeneous solid metal, its effective areal impedance can be written as

$$Z_e = \frac{1}{\sigma_e \delta} = R_e - i\omega L_e,$$

where δ is the skin depth, characteristic for a constitutive metal. The effective areal electronic resistance $R_e = m\nu_e/(e^2\delta N_e)$ determines the amount of power absorbed on the metal surface, and the areal reactance $-\omega L_e$ determined by kinetic electronic inductance $L_e = m/(e^2\delta N_e)$ accounts for the phase shift between the electric field and surface current induced in the surface skin layer.

For a metallic nanoporous surface, we also have to account for the effective areal capacitance in order to describe the charge accumulation in the void boundaries. We describe plasma oscillations of the lth mode in the lattice of voids by an equivalent *RLC* circuit composed of the equivalent areal capacitance C_l connected in parallel to the $R_l L_l$ branch (see Fig. 1). The equivalent impedance of this circuit can be written as

$$Z_l = \frac{R_l - i\omega L_l}{1 - \omega^2 L_l C_l - i\omega R_l C_l}. \tag{1}$$

Here $R_l = 2m\nu_l/(e^2\Delta_l\delta N_e)$ is the equivalent areal electronic resistance and $L_l = m/(e^2\Delta_l\delta N_e)$ is the areal kinetic electronic inductance characteristic of the lth plasmon mode, where ν_l is the damping of the lth plasmon mode due to all dissipative processes except radiative damping, and Δ_l is the fraction of free electrons participating in the plasma oscillations at the lth mode. We estimate the equivalent areal capacitance as $C_l = |f_l|^2 d\varepsilon_0$, where d is the void diameter, ε_0 is the electrical constant, $|f_l|^2$ is the dimensionless phenomenological form factor characteristic of a given lth multipole plasmon mode of a void, which is a free parameter in this simple model. Substituting the expressions for R_l, L_l, and C_l given above in Eq. (1), one finds

$$Z_l = \frac{m}{e^2\Delta_l\delta N_e}\frac{\omega_l^2(2\nu_l - i\omega)}{(\omega_l^2 - \omega^2 - 2i\omega\nu_l)},$$

where

$$\omega_l = \frac{1}{\sqrt{L_l C_l}} = \sqrt{\frac{e^2\Delta_l\delta N_e}{|f_l|^2 d\varepsilon_0 m}} \tag{2}$$

is the frequency of the lth plasmon mode. In the vicinity of the resonance, $\omega \simeq \omega_l$, assuming that $2\nu_l \ll \omega_l$, we finally obtain

$$Z_l \simeq -\frac{1}{2} i \frac{m}{e^2\Delta_l\delta N_e}\frac{\omega_l^2}{(\omega_l - \omega - i\nu_l)}.$$

With this consideration, we can easily obtain the total frequency-dependent equivalent areal impedance of the 2D lattice of voids in the form

$$Z_{\text{eff}} \simeq \frac{m}{e^2\delta N_e}(\nu_e - i\omega) - i\frac{m}{2e^2}\sum_{l=1}^{\infty}\frac{|\beta_l|^2}{\Delta_l\delta N_e}\frac{\omega_l^2}{(\omega_l - \omega - i\nu_l)}, \tag{3}$$

where $|\beta_l|^2 < 1$ is the phenomenological coefficient of coupling between the external oscillating electric field $\mathbf{E}\exp(-i\omega t)$ and the lth plasmon mode, which depends on the geometry of the particular structure under consideration. The first term in Eq. (3) describes the Drude response of homogeneous portions of the metal within intervoid regions to the external field.

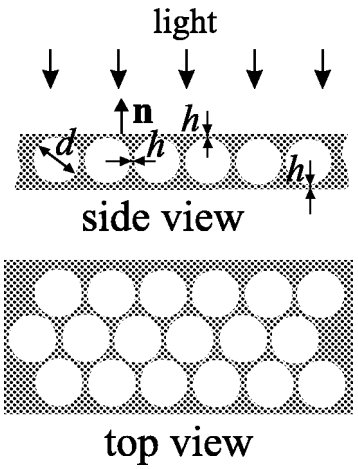

FIG. 2. Nanoporous metal film containing an hexagonal lattice of spherical voids. The void-to-surface distance h is chosen to be equal to the intervoid spacing.

In the vicinity of the lth plasma resonance, $\omega \simeq \omega_l$, the lth term of the summation dominates the right-hand side of Eq. (3) and we have

$$Z_{\text{eff}} \approx -i \frac{m|\beta_l|^2}{2e^2 \Delta_l \delta N_e} \frac{\omega_l^2}{(\omega_l - \omega - i\nu_l)}. \tag{4}$$

B. Porous metal film suspended in vacuum

Consider an external electromagnetic plane wave incident normally onto the metal porous film containing the 2D lattice of voids and suspended in vacuum (Fig. 2). We describe the metal porous film by an equivalent sheet with the effective surface impedance Z_{eff} obtained in the previous subsection. Obviously, the phenomenological coupling parameter $|\beta_l|^2$ depends on the void-to-surface distance h in such a structure. We solve the Maxwell equations in the surrounding media with the boundary conditions for electric **E** and magnetic **H** fields in the form

$$\begin{gathered} \mathbf{E}_{\text{in}} + \mathbf{E}_{\text{rf}} = \mathbf{E}_{\text{tr}}, \\ \mathbf{E}_{\text{in}} + \mathbf{E}_{\text{rf}} = Z_{\text{eff}}[\mathbf{n} \times (\mathbf{H}_{\text{in}} + \mathbf{H}_{\text{rf}} - \mathbf{H}_{\text{tr}})], \end{gathered} \tag{5}$$

where subscripts in, rf, and tr refer to the incident, reflected, and transmitted waves, respectively, and **n** is the external normal to upper planar surface of the metal film (see Fig. 2). As a result, we obtain the complex amplitude reflection and transmission coefficients as[15]

$$r = -\frac{Z_0}{2Z_{\text{eff}} + Z_0}, \quad t = \frac{2Z_{\text{eff}}}{2Z_{\text{eff}} + Z_0}, \tag{6}$$

where Z_0 is the free-space impedance.

The surface impedance given by Eq. (4) leads to the following expressions for the reflectance, transmittance, and absorbance of light in the neighborhood of the lth plasma resonance:

$$\begin{gathered} R = rr^* \approx \frac{\nu_l^2 + (\omega_l - \omega)^2}{(\omega_l - \omega)^2 + (\nu_l + \gamma_l^{(\text{f})})^2}, \\ T = tt^* \approx \frac{(\gamma_l^{(\text{f})})^2}{(\omega_l - \omega)^2 + (\nu_l + \gamma_l^{(\text{f})})^2}, \\ A = 1 - R - T \approx \frac{2\nu_l \gamma_l^{(\text{f})}}{(\omega_l - \omega)^2 + (\nu_l + \gamma_l^{(\text{f})})^2}, \end{gathered} \tag{7}$$

where

$$\gamma_l^{(\text{f})} = |\beta_l^{(\text{f})}|^2 \frac{m\omega_l^2}{Z_0 e^2 \Delta_l \delta N_e}. \tag{8}$$

If we ignore electron scattering in metal ($\nu_l = 0$), then the full linewidth of the lth resonance would be given by the value of $\gamma_l^{(\text{f})}$; correspondingly, $\gamma_l^{(\text{f})}$ describes the radiative broadening of the plasma resonance.

It should be noted that the transmission and absorption resonances have Lorentzian line shape with full width at half maximum (FWHM) $2(\nu_l + \gamma_l^{(\text{f})})$. The free parameters $|f_l^{(\text{f})}|^2/\Delta_l$ and $|\beta_l^{(\text{f})}|^2/\Delta_l$ can be obtained by fitting the resonance frequency and FWHM yielded by this simple model of resonant porous metal film to those obtained by a self-consistent electromagnetic model, which is done in Sec. IV of this paper.

At resonance, $\omega = \omega_l$, one finds

$$\begin{gathered} T_{\text{res}} = \frac{(\gamma_l^{(\text{f})})^2}{(\nu_l + \gamma_l^{(\text{f})})^2}, \quad R_{\text{res}} = \frac{\nu_l^2}{(\nu_l + \gamma_l^{(\text{f})})^2}, \\ A_{\text{res}} = 1 - R_{\text{res}} - T_{\text{res}} = \frac{2\nu_l \gamma_l^{(\text{f})}}{(\nu_l + \gamma_l^{(\text{f})})^2}. \end{gathered} \tag{9}$$

It is readily seen that $A_{\text{res}} \leqslant 0.5$ for any values of $\gamma_l^{(\text{f})}$ and ν_l. The maximum value, $A_{\text{res}} = 0.5$, occurs when $\gamma_l^{(\text{f})} = \nu_l$. The transmittance T also grows at the resonance and reaches a value 0.25, while the reflectivity R drops down to the same value of 0.25. This means that in the case of a symmetric environment the nanoporous metal film reradiates the energy of incident light equally into each surrounding medium, as it should when light is coupled to a resonance in a symmetric system like our film.

Formula (8) suggests that the radiative damping $\gamma_l^{(\text{f})}$ itself may be conceived as the coupling coefficient that controls the strength of interaction between the plasmon mode and light. Note that the role of radiative damping as a coupling coefficient describing the interaction between the eigenoscillations and external radiation has been shown for different open electromagnetic systems: plasmons[16] and cyclotron polaritons[17,18] in 2D electron systems, exciton polaritons in quantum wells,[19] and plasmons in metallic nanoshells.[8] For small $\gamma_l^{(\text{f})}$, $\gamma_l^{(\text{f})} \ll \nu_l$, this coupling is weak and the plasmon mode absorbs light poorly. In the opposite limit, $\gamma_l^{(\text{f})} \gg \nu_l$, the strong plasma-oscillation currents that flow on the metal film surfaces reradiate incident light back into the surrounding media, which again reduces absorption drastically. In the intermediate case, it is possible to realize the condition of maximum absorption of light by plasmons in porous metal

films by choosing a specific value of the coupling coefficient $|\beta_l^{(f)}|^2$, which yields $\gamma_l^{(f)}=\nu_l$. The optimal value of $|\beta_l|^2$ can be easily realized for voidlike plasmon modes in the spherical voids buried in metal. For example, the condition $\gamma_l=\nu_l$ can be easily satisfied for voidlike plasmons in a metallic nanoshell by choosing a specific value of the shell-layer thickness, as shown in Ref. 8.

C. Porous metal film supported by the bulk metal substrate

Now let us consider an electromagnetic plane wave incident from vacuum normally onto a planar surface of bulk metal that contains a 2D lattice of voids just beneath the surface. In this case $\mathbf{E}_{tr}$ and $\mathbf{H}_{tr}$ vanish in Eq. (5) and one obtains the impedance boundary condition[20]

$$\mathbf{E}_{in}+\mathbf{E}_{rf}=Z_{eff}[\mathbf{n}\times(\mathbf{H}_{in}+\mathbf{H}_{rf})]. \tag{10}$$

Solving Maxwell's equations in the ambient medium (vacuum) together with boundary condition equation (10), it is easy to obtain the complex amplitude reflection coefficient

$$r=\frac{Z_{eff}-Z_0}{Z_{eff}+Z_0}. \tag{11}$$

The surface impedance given by Eq. (4) leads to the following expression for the reflectance and absorbance of light in the neighborhood of the lth plasma resonance:

$$R=rr^*\approx\frac{(\omega_l-\omega)^2+(\gamma_l^{(s)}-\nu_l)^2}{(\omega_l-\omega)^2+(\gamma_l^{(s)}+\nu_l)^2},$$
$$A=1-R\approx\frac{4\nu_l\gamma_l^{(s)}}{(\omega_l-\omega)^2+(\gamma_l^{(s)}+\nu_l)^2}. \tag{12}$$

Here

$$\gamma_l^{(s)}=|\beta_l^{(s)}|^2\frac{m\omega_l^2}{2Z_0e^2\Delta_l\delta N_e} \tag{13}$$

is the radiative damping of the lth plasmon mode on the nanoporous metal surface. Comparing Eqs. (8) and (13) one can see that the radiative broadening of the plasma resonance in the nanoporous metal film is twice of that at the nanoporous metal surface, $\gamma_l^{(f)}=2\gamma_l^{(s)}$ (under the assumption that the coupling coefficient $|\beta_l|^2$ is the same in both cases), because void plasmons in the film reradiate into either surrounding medium. The absorption resonance described by Eq. (12) has a Lorentzian line shape with FWHM $2(\nu_l+\gamma_l^{(s)})$. Again, the free parameters $|f_l^{(s)}|^2/\Delta_l$ and $|\beta_l^{(s)}|^2/\Delta_l$ can be obtained by fitting the resonance frequency and FWHM yielded by this simple model of resonant porous metal surface to those obtained by a self-consistent electromagnetic model, which is done in Sec. IV of this paper.

Finally, at resonance, $\omega=\omega_l$, one finds

$$R_{res}\approx\frac{(\gamma_l^{(s)}-\nu_l)^2}{(\gamma_l^{(s)}+\nu_l)^2},$$
$$A_{res}\approx\frac{4\nu_l\gamma_l^{(s)}}{(\gamma_l^{(s)}+\nu_l)^2}.$$

It is readily seen that nearly total light absorption by the lth plasmon mode ($A_{res}\approx1$) occurs when $\nu_l=\gamma_l^{(s)}$, while the reflectivity, R_{res}, drops down to zero.

III. SELF-CONSISTENT ELECTROMAGNETIC MODEL: SCATTERING-MATRIX LAYER-KKR APPROACH

Here we consider a more specific periodic 2D hexagonal lattice of spherical voids inside a metal with primitive lattice vectors $\mathbf{a}$ and $\mathbf{b}$, where $|\mathbf{a}|=|\mathbf{b}|$ and $\mathbf{a}\cdot\mathbf{b}=|\mathbf{a}|^2\cos 60°$. The lattice of voids may reside inside a planar metal film or may be buried beneath the planar surface of bulk metal. We assume that external light shines normally onto the planar surface of the metal.

To calculate light absorption in such a porous structure we use a rigorous solution of Maxwell's equations based upon a multiple-scattering layer-KKR approach that makes use of a reexpansion of the plane-wave representation of the electromagnetic field in terms of spherical harmonics.[12–14,21,22] This approach involves the following steps. First, we divide the whole structure into parts separated by parallel planes that form two homogeneous semi-infinite media and a planar layer in between that contains the periodic lattice of voids. This periodic layer may be formed either by the actual planar porous metal film or by a porous layer beneath the surface of bulk metal. In the latter case, the homogeneous semi-infinite space below the periodic layer is filled with the homogeneous metal medium. The periodic layer is treated within the KKR method in a spherical-wave representation, whereas the interaction between the field in the periodic layer and the field in the homogeneous semispaces is treated separately in a plane-wave representation.

One of the advantages of this scattering-matrix approach is that it employs explicitly the decomposition of the total field into a sum of waves propagating (or decaying) along and counter to the $\mathbf{n}$ direction (see Fig. 2). It allows one to avoid difficulties with convergence when describing the evanescent waves. The total fields in the homogeneous media surrounding the periodic metal layer result from the superposition of propagating (and evanescent) plane waves

$$\mathbf{E}_{tot}^{\pm}=\sum_g\mathbf{E}_g^{\pm}\exp(i\mathbf{K}_g^{\pm}\cdot\mathbf{r})$$

with transverse wave vectors

$$\mathbf{K}_g^{\pm}=[\mathbf{g},\pm\sqrt{k^2-\mathbf{g}^2}],$$

where $k=k_0\sqrt{\varepsilon(\omega)}$ inside the metal, $k=k_0$ is the momentum of light in the surrounding vacuum, $\mathbf{g}=p\mathbf{A}+q\mathbf{B}$ are the in-plane reciprocal lattice vectors, $\mathbf{A}=2\pi(\mathbf{b}\times\mathbf{n})/|\mathbf{a}\times\mathbf{b}|$ and $\mathbf{B}=2\pi(\mathbf{n}\times\mathbf{a})/|\mathbf{a}\times\mathbf{b}|$ are the primitive vectors of the reciprocal 2D lattice, p and q are integers, and $\mathbf{r}$ is the radius vector. The superscripts $+$ and $-$ label waves that propagate (or decay) along and counter to the $\mathbf{n}$ direction, respectively. The square root of the frequency-dependent dielectric function $\varepsilon(\omega)$ is chosen here to have a non-negative imaginary

part. It should be noted that every plane wave in the metal substrate is evanescent at frequencies below the bulk plasma frequency.

The total field inside the layer with a periodic lattice of voids is represented as a superposition of the incoming plane waves (both propagating and evanescent) and the field scattered from every void,

$$\mathbf{E}_{\mathrm{sc}}(\mathbf{r}) = \sum_{l} \sum_{m=-l}^{l} \left(\frac{i}{k} b_{lm}^{E} \boldsymbol{\nabla} \times \sum_{\mathbf{R}_n} h_l^{+}(kr_n) \mathbf{X}_{lm}(\hat{\mathbf{r}}_n) + b_{lm}^{H} \sum_{\mathbf{R}_n} h_l^{+}(kr_n) \mathbf{X}_{lm}(\hat{\mathbf{r}}_n) \right), \tag{14}$$

where $h_l^{+}(kr)$ is the spherical Hankel function of lth order, which has the asymptotic form describing an outgoing spherical wave $h_l^{+}(kr) \approx (-i)^l \exp(ikr)/ikr$ at $r \to \infty$; $\mathbf{r}_n = \mathbf{r} - \mathbf{R}_n$; $\mathbf{R}_n$ is the radius vector of the center of the nth void; $\mathbf{X}_{lm}(\hat{\mathbf{r}})$ is a vector spherical harmonic defined by

$$\sqrt{l(l+1)}\mathbf{X}_{lm}(\hat{\mathbf{r}}) = -i\hat{\mathbf{r}} \times Y_{lm}(\hat{\mathbf{r}}),$$

where the unit vector $\hat{\mathbf{r}}$ denotes the angular variables (θ, ϕ) of the radius vector $\mathbf{r}$ in spherical coordinates and Y_{lm} are spherical harmonics. The amplitude coefficients $b_{lm}^{E,H}$ of the scattered spherical waves with E and H polarizations in Eq. (14) are determined using the scattering matrix of a void that relates the total electromagnetic field incident upon a given single void with the electromagnetic field scattered from this void:

$$\begin{pmatrix} \mathbf{b}^{E} \\ \mathbf{b}^{H} \end{pmatrix} = \begin{pmatrix} \mathbf{T}^{E} & 0 \\ 0 & \mathbf{T}^{H} \end{pmatrix} \begin{pmatrix} \mathbf{a}^{E} \\ \mathbf{a}^{H} \end{pmatrix}, \tag{15}$$

where $\mathbf{b}^{E,H} \equiv \{b_{lm}^{E,H}\}$ are the column matrices of $l_{\max}(l_{\max}+2)$ elements, $\mathbf{a}^{E,H} \equiv \{a_{lm}^{E,H}\}$ are the column matrices with the amplitude coefficients of the combined electromagnetic field incident upon a given single void as their elements, $l_{\max}$ is cutoff value of the angular momentum in the spherical-wave expansion to reach a desired level of convergence. The elements of the scattering matrices of spherical voids depend only on l as

$$T_{lm;l'm'}^{E,H} = T_{l}^{E,H} \delta_{ll'} \delta_{mm'},$$

where[13,23]

$$T_l^{E} = \frac{-\varepsilon(\omega) j_l(\rho_1)[\rho_0 j_l(\rho_0)]' + [\rho_1 j_l(\rho_1)]' j_l(\rho_0)}{\varepsilon(\omega) h_l^{+}(\rho_1)[\rho_0 j_l(\rho_0)]' - [\rho_1 h_l^{+}(\rho_1)]' j_l(\rho_0)},$$

$$T_l^{H} = \frac{-j_l(\rho_1)\rho_0 j'_l(\rho_0) + \rho_1 j'_l(\rho_1) j_l(\rho_0)}{h_l^{+}(\rho_1)\rho_0 j'_l(\rho_0) - \rho_1 [h_l^{+}(\rho_1)]' j_l(\rho_0)}, \tag{16}$$

$\rho_0 = k_0 d/2$, $\rho_1 = k_0 d\sqrt{\varepsilon(\omega)}/2$, and the prime denotes differentiation with respect to the argument.

The field scattered from each void reaches out other voids and contributes to the their scattered fields. The layer-KKR method incorporates this effect by translating outgoing spherical waves from each void to other voids, where they are expressed as spherical components of plane waves. The details of this translation procedure have been taken from Ref. 12. Then, a summation has to be performed over all of these in-plane scattering contributions, which is performed directly in real space in our case, since the metal provides a natural space cutoff distance beyond which the voids cannot *see* each other through the intervoid metal portions.

Therefore, we have decomposed the combined field incident upon a given single void into spherical waves that are scattered according to the above equations. Then, we transform the combined field scattered from all voids into the plane-wave representation that is expressed as a sum over in-plane reciprocal vectors $\mathbf{g}$,

$$\mathbf{E}_{\mathrm{sc}}^{\pm} = \sum_{g} [\mathbf{E}_{\mathrm{sc}}^{\pm}]_g \exp(i\mathbf{K}_g^{\pm} \cdot \mathbf{r}),$$

and apply the boundary conditions at the interfaces of the layer containing the lattice of voids with the surrounding media. As a result we construct the scattering matrix of the entire structure, which allows us to calculate the reflectance, R, transmittance, T, and absorpbance, $A = 1 - R - T$, of the entire structure. This procedure is explained in great detail in Ref. 12, together with the extension to an arbitrary number of layers is done.

It is interesting to point out that, even if different voids in the lattice are close packed, they are only weakly coupled through the metal, so that each void interacts directly only with its nearest neighbors. Accordingly, the Bragg resonances controlled by the periodicity of the system are not exhibited in the calculated spectra. Therefore, only resonances originating in the excitation of Mie plasmon modes in every single void influenced by nearest void neighbors show up in the spectra.

In our calculations we assume that the intervoid spacing along the lattice vectors $\mathbf{a}$ and $\mathbf{b}$ is equal to the void-to-surface distance h (see Fig. 2). Below we present the results of numerical calculations performed with $l \leqslant 12$ and up to 151 g's, which ensure that our calculations are closer than 1% with respect to the converged ones.

IV. OPTICAL SPECTRA OF NANOPOROUS STRUCTURES

A. Drude model

In this section, we describe the dielectric response of the metal to an electric field $\mathbf{E}\exp(-i\omega t)$ in the local Drude model as

$$\varepsilon(\omega) = 1 - \frac{\omega_p^2}{\omega(\omega + i\nu_e)},$$

where ω_p is the bulk plasmon frequency and ν_e is a phenomenological bulk electron relaxation rate. For our calculations we chose the parameters $\omega_p = 8.7$ eV and $\nu_e = 45$ meV,[24] which are characteristic for silver.

Figure 3(a) shows the calculated absorption spectra of light incident normally onto an unsupported silver film containing a single hexagonal lattice of voids. The absorption of light grows resonantly at the frequencies of plasma resonances in nanovoids when the void-to-surface distance h is of the order of the skin depth (which is about 23 nm for silver). The maximum resonant light absorption, $A_{\mathrm{res}} = 0.5$,

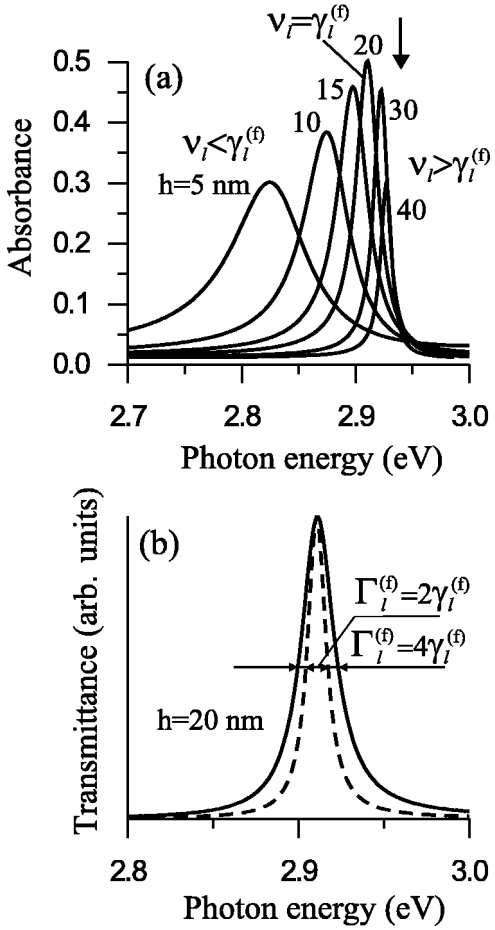

FIG. 3. Optical spectra of light incident normally onto a planar silver film with an hexagonal lattice of spherical voids of diameter $d=300$ nm. The metal is described by dielectic function in the Drude model (see text). (a) Variation of the absorption spectra with void-to-surface distance h, which is chosen to be equal to the intervoid spacing. The vertical arrow marks the energy of the fundamental plasmon mode of a single void in bulk silver. (b) Transmission spectra calculated by taking into account electron relaxation, $\nu_e=45$ meV (solid curve), and without electron relaxation (dashed curve). The void-to-surface distance $h=20$ nm produces an absorption maximum (50%) at resonance [see (a)]. Curves are normalized to have the same height for comparison sake.

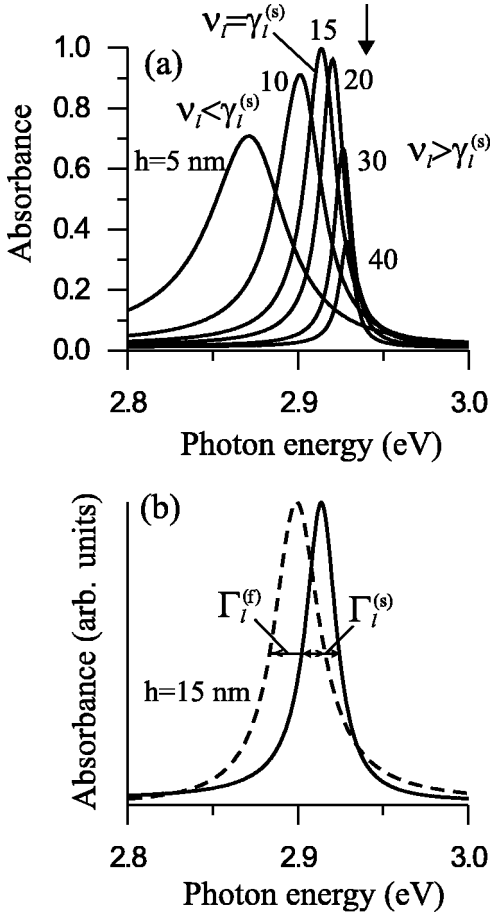

FIG. 4. (a) Absorption spectra of light incident normally onto a planar nanoporous silver surface with an hexagonal lattice of spherical voids of 300 nm in diameter beneath the surface for different values of void-to-surface distance h, which is chosen to be equal to the intervoid spacing. The metal is described by the dielectic function in the Drude model. The vertical arrow marks the energy of the fundamental plasmon mode of a single void in bulk silver. (b) Light absorption spectra by a nanoporous silver film suspended in vacuum (dashed line) and a nanoporous silver surface (solid line) for the same parameters: $d=300$ nm and $h=15$ nm. Curves are normalized to have the same height for comparison sake. The FWHM's of these two resonance curves are interrelated by $\Gamma_l^{(f)}=3\Gamma_l^{(s)}/2$.

occurs when $h=20$ nm. Although the frequency of the plasma resonance in the porous metal film is close to the frequency of the fundamental (the orbital quantum number, l, is unity) Mie plasmon mode of a single spherical void in an infinite metallic medium, they do not coincide. As clearly seen in Fig. 3(a), the shift between these two frequencies grows with decreasing the intervoid spacing, which shows that the reason for such a shift is the coupling of plasmons in adjacent voids. It should be noted that the linewidth of plasma resonance gradually increases with decreasing void-to-surface distance, i.e., increase of the coupling parameter $|\beta_l|^2$ due to growing radiative contribution to the linewidth.

In Fig. 3(b) we compare the light transmission spectrum of the nanoporous silver film in the case of maximum light absorption (50% at resonance) with the transmission spectrum of the same film calculated by neglecting electron relaxation in the metal ($\nu_e=0$). The curves are normalized to have the same height for the sake of comparison. Without electron relaxation taking into account, the FWHM of the transmission resonance is entirely of the radiative origin, and hence, the FWHM is equal to $2\gamma_l^{(f)}$ in this case (see relevant discussion in Sec. II). The FWHM of the transmission resonance curve corresponding to the maximum light absorption is exactly twice broader. This is proof of the criterion derived in Sec. II in the framework of a simple equivalent model, which proposes that the maximum absorption at plasma resonance occurs when the radiative and dissipative broadening of the resonance equal each other.

Figure 4(a) shows the calculated absorption spectra of light incident normally onto a nanoporous silver surface (nanoporous silver film supported by the bulk silver sub-

strate). Again the light absorption exhibits resonant enhancement at the frequencies of nanovoid plasma resonances. The total resonant light absorption predicted by the simple model of Sec. II occurs when the lattice of spherical voids is buried in the metal substrate at a specific distance from the metal surface, which ensures optimal coupling of void plasmons to the external light. Remarkably, *even a single* lattice of nanovoids beneath the planar metal surface can produce the total light absorption on such a nanoporous metal surface, whereas this surface is highly reflective away from the plasma resonance.

Comparing Figs. 3(a) and 4(a) one can see that the void-to-surface distance producing the maximum light absorption is less for the nanoporous surface [Fig. 4(a)]. This is due to the smaller radiative damping inherent in near-surface lattices of voids as compared to that in the metal film [cf. Eqs. (8) and (13)]. Therefore, to satisfy the condition of optimal coupling between light and void plasmons at nanoporous metal surface, $\gamma_l^{(s)}=\nu_l$, one should place the lattice of voids closer to the metal surface in order to increase the value of the coupling parameter $|\beta_l|^2$.

It is worth noting that the FWHM of resonant curves with maximum absorption at resonance are very close to each other in either structure: the nanoporous metal film ($h=20$ nm) and nanoporous metal surface ($h=15$ nm). Taking into account this fact and the condition of optimal coupling $\gamma_l^{(f,s)}=\nu_l$ obtained in Sec. II, one can conclude that the dissipative broadening of plasma resonances is almost the same for both structures, which suggests that void-plasmon fields are strongly confined inside the voids, so that the void-to-surface distance does not influence much the dissipative broadening of the resonance.

In Fig. 4(b) the absorption spectra of light are shown for our two different structures: a nanoporous silver film suspended in vacuum (dashed line) and a nanoporous silver surface (solid line) for the same parameters d and h. The void-to-surface distance $h=15$ nm in Fig. 4(b) corresponds to the maximum absorption ($\approx 100\%$) at resonance in Fig. 4(a), where $\gamma_l^{(s)}=\nu_l$. One can see that the FWHM of the plasma resonance in the nanoporous film is by 50% broader than that on the nanoporous metal surface. The FWHM of resonance curve is given by $\Gamma_l^{(s,f)}=2(\nu_l+\gamma_l^{(s,f)})$. Because the dissipative broadening of the resonance is almost the same in both structures as deduced above we have $\gamma_l^{(f)}=2\gamma_l^{(s)}$, which yields $\Gamma_l^{(f)}=3\Gamma_l^{(s)}/2$ [see Fig. 4(b)]. This consideration confirms the conclusion drawn in Sec. II: the radiative broadening of plasma resonance in the nanoporous film is twice as much as that at nanoporous metal surface for the same void-to-surface distance (i.e., the same coupling coefficient $|\beta_l|^2$) for both structures.

Now, we can estimate the free parameters $|f_l|^2/\Delta_l$ and $|\beta_l|^2/\Delta_l$ introduced in Sec. II by fitting Eqs. (2), (8), and (13) to the resonance frequency and FWHM in the case of maximum light absorption at resonance. As it was shown in Sec. II the FWHM acquires the value of $4\gamma_l^{(f,s)}$ in this case [solid lines in Figs. 3(b) and 4(b)]. In these calculations we assume $\delta=23$ nm and $N_e=5.86\times 10^{22}$ cm^{-3} for silver. We obtain the free parameters $|f_l^{(f,s)}|^2/\Delta_l\approx 0.6$, $|\beta_l^{(f)}|^2/\Delta_l\approx 0.07$ and $|\beta_l^{(s)}|^2/\Delta_l\approx 0.13$. The form-factors $|f_l^{(f)}|$ and $|f_l^{(s)}|$ are very close to each other because the positions of resonances of the plasmon Mie modes localized in voids do not depend essentially on the void-to-surface distance. As expected, the coupling coefficient $|\beta_l^{(s)}|^2$ for the nanoporous metal surface is almost twice as much as that for the nanoporous metal film, $|\beta_l^{(f)}|^2$.

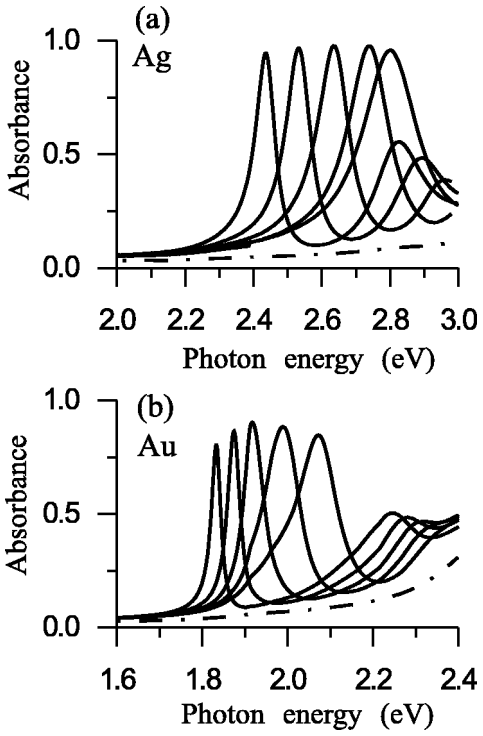

FIG. 5. Absorption spectra of light incident normally onto planar (a) silver and (b) gold surfaces with a lattice of spherical voids right beneath it (see Fig. 2). The metal is described by dielectic function based upon experimental optical constant data (Ref. 26). The plots show the variation of the spectra with the void diameter for an intervoid spacing $h=5$ nm, chosen to be equal to the void-to-surface distance. The void diameter is (from right to left) (a) 260, 300, 320, 340, and 360 nm; (b) 420, 440, 460, 480, 500 nm. The absorption of light on the homogeneous surfaces of bulk silver (a) and gold (b) is shown by dash-dotted curves.

B. Dielectric function of metal based upon experimental data

We have described the dielectric response of the metal by the simple Drude model in the previous subsection to reveal essential physics of light-plasmon interaction in two different nanoporous structures. However, as seen from Figs. 3 and 4, the frequencies of plasma resonances in the structures under consideration fall rather close to the interband absorption edge (3.5 eV for silver[25]). In this frequency range the Drude model becomes inaccurate and direct experimental optical data should be used to describe the dielectric response of the metal.

Figure 5 shows the calculated absorption spectra of light incident normally onto nanoporous silver and gold surfaces with a single periodic layer of close-packed voids buried beneath the surface for different void diameters. Hereafter, we use experimental optical data[26] to describe the dielectric

function of silver and gold in our calculations. Almost total resonant light absorption occurs when the lattice of voids is buried in a silver substrate at distances smaller than the skin depth [Fig. 5(a)] and rather high resonant absorption occurs on the nanoporous gold surface [Fig. 5(b)].

It should be noted that resonant absorption decreases with deviation of the void diameter from the optimal value (Fig. 5). The reason is that the variation of the void diameter changes the radiative damping of void plasmons and hence breaks the condition of optimal coupling ($\gamma_l^{(s)} = \nu_l$) between light and plasmons. This fact is consistent with radiative damping calculations performed for plasmons in metallic nanoshell,[8] where the increasing of shell-core diameter leads to a decrease in the radiative damping of voidlike plasmons in nanoshells. Our calculations show that the absorption spectra are independent of the polarization of normally incident light by virtue of the hexagonal symmetry of the void lattice.

Figure 5 depicts the spectra of resonant absorption of light caused by the excitation of the fundamental Mie plasmon mode ($l=1$) in voids. The frequencies of high-order plasma resonances fall within the interband absorption spectra (at frequencies higher than 3.5 eV for silver and 2.2 for gold[25]), and therefore, these resonances can hardly be observed in the reflectivity spectra. The frequencies of plasma resonances at a nanoporous metal surface can be reduced by filling the pores with a dielectric material. Figure 6 shows the calculated absorption spectra of light incident normally onto silver and gold surfaces with filled spherical nanopores. In this case the second and the third plasmon resonances along with the fundamental plasma resonance show up in the visible. As seen in Fig. 6 a giant light absorption can also be achieved at high-order plasma resonances.

We can estimate the local-field enhancement factor at plasma resonances as $|f| = \omega_{\mathrm{res}}/\Gamma$, where ω_{res} is the resonance frequency and Γ is the FWHM of the resonance. The height of the resonance peaks in Fig. 6 is measured from the smooth nonresonant background contribution. The local-field enhancement factors exceeding 50 and 70 are reached at plasma resonances at silver and gold surfaces with dielectric spherical inclusions, respectively, which are shown in Fig. 6. Even greater local field enhancement factors (up to 85) can be achieved at the nanoporous silver surface for deeper location of the void lattice in the silver substrate (for the void-to-surface distance $h=20$ nm). Notice for comparison that the local-field enhancement factor obtained at plasma resonances in a gold solid nanosphere is below 15.[1,2] In general, much greater field enhancement is characteristic of the plasmons on metal surfaces with negative curvature. For example, it was shown in Ref. 8 that ultrahigh values of the local-field enhancement factor exceeding 60 and 150 for gold and silver nanoshells, respectively, can be achieved at voidlike plasmon resonance for specific values of shell-layer thickness.

Close-packed segment void structures with different segment depths have been studied experimentally.[3–5] Although the geometry studied in our paper is not that of segment voids, our theoretical results for voids completely buried in metal unambiguously show that in every nanoporous metal structure a specific optimal value of light-plasmon coupling

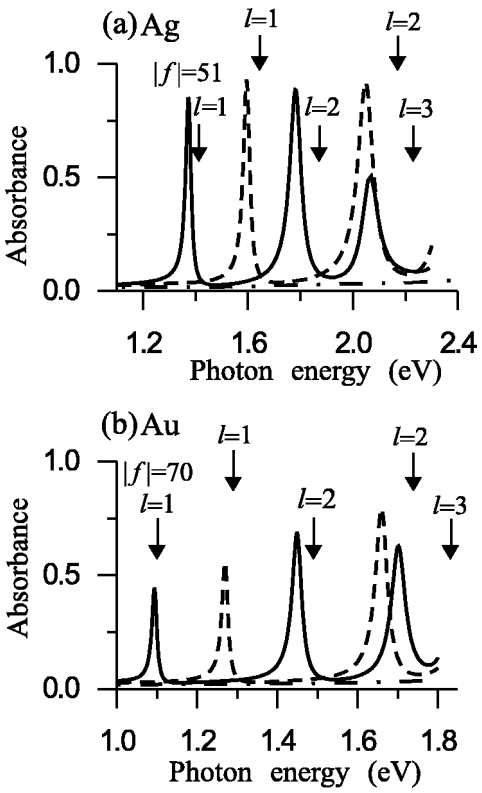

FIG. 6. Absorption spectra of light incident normally onto silver (a) and gold (b) surfaces with a lattice of spherical inclusions of a material with dielectric constant $\varepsilon=4.5$ (solid curves) and $\varepsilon=3.3$ (dashed curves). The void-to-surface distance h is equal to 5 nm and diameter of spherical inclusions d is 300 nm (a) and 400 nm (b). The absorption of light on homogenous surfaces of bulk silver and gold is shown by dash-dotted curves. The vertical arrows mark the energies of the fundamental ($l=1$), second ($l=2$), and third ($l=3$) plasmon Mie modes of a single void in respective bulk metal.

(depending on the void-to-surface distance) exists producing the maximum light absorption, similar to the results found in experiment.

V. CONCLUSIONS

We have shown theoretically that nanoporous metals exhibit remarkable resonant absorption properties. Nearly total light absorption on a nanoporous surface of metal can be achieved at the plasma resonance. This phenomenon occurs when the lattice of spherical voids is buried in the metal substrate at a specific distance from the metal surface, which ensures optimal coupling of plasmons in the voids to the external light. Based upon a simple model, corroborated by detailed calculations later on, we have found a physical criterion for the optimal coupling, which proposes that the radiative broadening of the plasma resonance must be equal to its dissipative broadening in order to produce maximum light absorption at the resonance. It is worth mentioning that the resonant light absorption by void plasmons is accompanied by high local-field enhancement. This could be used to trigger nonlinear effects.[27] The frequencies of plasma resonances can be easily tuned by varying the diameter of the voids or

by filling them with dielectric materials. This makes this type of nanoporous metals a very attractive choice for a variety of applications ranging from nanophotonics to biophysics.

ACKNOWLEDGMENTS

We thank J. J. Baumberg, V. G. Golubev, and S. G. Tikhodeev for inspiring conversations. This work was supported by the Russian Foundation for Basic Research (Grant No. 02-02-81031) and the Russian Academy of Science Program "Low-Dimensional Quantum Nanostructures." T.V.T. acknowledges the support from the President of Russia through the grant for young scientists MK-2314.2003.02 and from the National Foundation for Promotion of Science, and also thanks the Max Planck Institute for the Physics of Complex Systems in Dresden for hospitality during the preparation of this work. F.J.G.A. acknowledges help and support from the University of the Basque Country UPV/EHU (Contract No. 00206.215-13639/2001) and the Spanish Ministerio de Ciencia y Tecnología (contract No. MAT2001-0946).

[1] T. Klar, M. Perner, S. Grosse, G. von Plessen, W. Spirkl, and J. Feldmann, Phys. Rev. Lett. **80**, 4249 (1998).
[2] B. Lamprecht, J. R. Krenn, A. Leitner, and F. R. Aussenegg, Phys. Rev. Lett. **83**, 4421 (1999).
[3] S. Coyle, M. C. Netti, J. J. Baumberg, M. A. Ghanem, P. R. Birkin, P. N. Bartlett, and D. M. Whittaker, Phys. Rev. Lett. **87**, 176801 (2001).
[4] P. N. Bartlett, J. J. Baumberg, S. Coyle, and M. Abdelsalem, Faraday Discuss. **125**, 117 (2003).
[5] S. Coyle, G. V. Prakash, J. J. Baumberg, M. Abdelsalem, and P. N. Bartlett, Appl. Phys. Lett. **83**, 767 (2003).
[6] E. Prodan, P. Nordlander, and N. J. Halas, Chem. Phys. Lett. **368**, 94 (2003).
[7] E. Prodan, C. Radloff, N. J. Halas, and P. Nordlander, Science **302**, 419 (2003).
[8] T. V. Teperik, V. V. Popov, and F. J. García de Abajo, Phys. Rev. B **69**, 155402 (2004).
[9] S. V. Gaponenko, A. A. Gaiduk, O. S. Kulakovich, S. A. Maskevich, N. D. Strekal, O. A. Prokhorov, and V. M. Shelekhina, Pis'ma Zh. Eksp. Teor. Fiz. **74**, 343 (2001) [JETP Lett. **74**, 309 (2001)].
[10] N. Stefanou, A. Modinos, and V. Yannopapas, Solid State Commun. **118**, 69 (2001).
[11] A. Modinos, N. Stefanou, and V. Yannopapas, Opt. Express **8**, 197 (2001).
[12] N. Stefanou, V. Yannopapas, and A. Modinos, Comput. Phys. Commun. **113**, 49 (1998); **132**, 189 (2000).
[13] F. J. García de Abajo, Phys. Rev. B **60**, 6086 (1999).
[14] F. J. García de Abajo, Phys. Rev. Lett. **82**, 2776 (1999).
[15] M. Dressel and G. Grüner, *Electrodynamics of Solids* (Cambridge University Press, Cambridge, 2002).
[16] V. V. Popov, O. V. Polischuk, T. V. Teperik, X. G. Peralta, S. J. Allen, N. J. M. Horing, and M. Wanke, J. Appl. Phys. **94**, 3556 (2003).
[17] V. V. Popov, T. V. Teperik, and G. M. Tsymbalov, Pis'ma Zh. Eksp. Teor. Fiz. **68**, 200 (1998) [JETP Lett. **68**, 210 (1998)].
[18] V. V. Popov and T. V. Teperik, Pis'ma Zh. Tekh. Fiz. **27**, 42 (2001) [Tech. Phys. Lett. **27**, 3, 193 (2001)].
[19] V. V. Popov, T. V. Teperik, N. J. M. Horing, and T. Yu. Bagaeva, Solid State Commun. **127**, 589 (2003).
[20] J. D. Jackson, *Classical Electrodynamics* (Wiley, New York, 1975).
[21] J. Korringa, Physica (Amsterdam) **13**, 392 (1947).
[22] W. Kohn and N. Rostoker, Phys. Rev. **94**, 1111 (1954).
[23] C. Bohren and D. Hufmann, *Absorption and Scattering of Light by Small Particles* (Wiley, New York, 1998).
[24] I. R. Hooper and J. R. Sambles, Phys. Rev. B **65**, 165432 (2002).
[25] P. B. Johnson and R. W. Christy, Phys. Rev. B **6**, 4370 (1972).
[26] E. D. Palik, *Handbook of Optical Constants of Solids* (Academic Press, New York, 1985).
[27] U. Kreibig and M. Vollmer, *Optical Properties of Metal Clusters*, Vol. 25 of Springer Series in Material Science (Springer-Verlag, Berlin, 1995).